Received: 27 January 2021 | Revised: 05 March 2021 | Accepted: 01 April 2021
DOI: 10.22034/ecc.2021.270619.1129
Eurasian Chemical Communications
SAMI

FULL PAPER

Effects of graphene oxide (GO) nanoparticle and SDS on storage capacity of CO_2 in hydrate

Haniyeh Shamsin Beyranvand[a,*] |Hamid Sarlak[b]

[a]*MSc. Chemical Engineering Department, Abadan Petrochemical Company, Abadan, Iran*

[b]*PHd. Chemical Engineering Department, Persian Gulf Fajr Energy Co., Iran*

In this study, the effect of nanoparticle of graphene oxide and surfactant sodium dodecyl sulfate (sds) 400 ppm on the storage capacity of co2 in hydrate was investigated. A laboratory system was developed for hydrate formation experiments. The experiments were carried out in the range of pressure 36-40 bar, temperature range from 273.35 k to 278.65 k, in the presence of graphene oxide and sodium dodecyl sulfate. Experimental results showed that by increasing the pressure at constant temperature for net water, storage capacity increased by 11%, and the storage capacity increased by 14% by decreasing the temperature at the constant pressure (36 bar). Adding sds increased storage capacity by 26%, while adding graphene oxide increased 4.2% of storage capacity. For this purpose, design expert software and response surface test method and historical method were used. Also, a mathematical equation was proposed to estimate the co2 storage capacity in hydrate.

***Corresponding Author:**
Haniyeh Shamsin Beyranvand
Email: Hani.shams94@gmail.com
Tel.: +989024672500

keywords

Storage capacity; sodium dodecyl sulfate; hydrate; graphene oxide.

Introduction

Carbon dioxide (CO_2) is one of the most effective greenhouse gases in global warming that plays a role in gradual increase in the Earth's temperature, contributing to 9% to 26% of the greenhouse effect [1,2]. As a method for separating and storing CO_2, hydration has drawn the attention of many researchers [3,4].

Generally found in the form of solid crystalline substances produced by hydrogen bonding in water, gas hydrates entrap gas molecules of lower molecular weight within a lattice [5]. As a unique feature, gas hydrates can hold about 180 times of the gas volume [6-9]. This high storage capacity has attracted attention in the industry. In addition, slow release of gas from hydrates, entrapment of flammable gases within the hydrates lattice, and their low storage pressure are other advantages of hydrates. However, they have not been used yet in the industry due to problems such as slow rate of hydrate formation for industrial applications, difficult separation and packaging of hydrate particles for transportation, and presence of unreacted water within the lattice which occupies a large percentage of volume within the hydrate lattice. Nevertheless, among the many methods of gas transmission and storage, gas hydrates can be of great interest because of their high storage capacity, possibility of gas transfer at moderately low temperatures and at ambient pressure, easy transfer at a lower cost, and easy production process. However, to produce them on an economic scale, one should consider problems such as high pressure and low formation rate, the need for increased stability, lower volume of gas

transport compared with other methods, and water separation [10-15]. Several solutions have been proposed in this regard. Accordingly, the present review addresses the use of nanoparticles and storage capacity enhancers. The former method can help prepare nanofluids to improve heat transfer in the hydrate formation system and provide suitable sites for heterogeneous nucleation of gas hydrates [16- 18]. The latter method can increase the solubility of the gas components in the water phase to improve their efficiency [19].

Babaee *et al.* (2018) investigated the kinetics of hydrate formation in a solution system of argon + tetra n butyl ammonium bromide + sodium dodecyl sulfate. They tested TBAB + WATER Ar + system and did kinetic studies and experiments in a reactor equipped with a high equilibrium agitator with an internal volume of approximately 340 cm at initial temperatures of 281, 285 and 287.5 K and initial pressures of 6.1, 1/8 and 10.1 MPa Done. The results showed that the induction time significantly decreased with increasing initial pressure. However, argon consumption also increased during hydrate formation. The same trend was identified and obtained by decreasing the initial temperature at a constant pressure. In addition, with increasing TBAB concentration, from 0.1 to 0.3 wt%, the rate of semi-clathrate hydrate nucleation and the amount of Ar consumption increased during hydrate formation, while induction time was significantly reduced. The results showed the positive kinetic effects of TBAB on Ar hydrates, indicating that TBAB is a reliable amplifier to increase the rate of argon hydrate formation. The results of adding SDS (at concentrations of 100 and 200 ppm) at an initial temperature of 285 K and initial pressures of 1.6 and 8.1 MPa show that SDS induced the formation of hemiclatrate hydrate for the Ar + o system. 1.1% wt TBAB + 0.9% wtH2O increased but there was no systematic relationship between induction time and SDS concentration for this system [19-21].

Airong Li *et al.* (2017) conducted a laboratory study of the formation of carbon dioxide using a reactor equipped with a stirrer containing induced gas. Carbon dioxide capture, storage and transportation technology is a creative idea and thinking. In this work, they conducted a laboratory study on the formation of CO_2 gas hydrate as a function of stirring and rotation speed of the reactor at different speeds from zero to 800 RPM, temperatures of 274.15 and 279.15 K and initial pressures from 2.1 to 6 MPa. They did it with the intended gas. The results showed that the formation of stable hydrate CO_2 (in the dissolution and nucleation stage) was significantly improved through a reactor equipped with a stirrer. As the stirrer speed increased, the induction time decreased from 261 to 24 revolutions per minute. Reactor design is one of the most important factors in the formation of CO_2 gas hydrate. In addition, the initial temperature and pressure had important effects on the storage capacity and formation of CO_2 hydrates. The induction time of nucleation (nucleation formation) was significantly reduced by decreasing the temperature and increasing the initial pressure from 185 minutes to 51 minutes. Also, the amount of mol of CO_2 consumed increased from 0.18 to 0.25 mol and the storage capacity increased [23].

Experimental

Materials

The carbon dioxide gas was used to check the purity of the experiments which was 99.99% purchased from the company Arvand Industrial Gases Co. The carbon dioxide gas cylinder has a volume of 50 liters and has an initial pressure of 42 MPa. Graphene oxide was purchased from the US Research Nanomaterials, Inc. And Sodium dodecyl sulfate (SDS) was used as the surfactant purchased from Merck Co.

Apparatus

For the experiment, a 316 (S-316) stainless steel jacketed reactor with an internal volume of 296 cm^3 was used, which had a bearing operating pressure of 200 bars. The internal chamber of the reactor was equipped with four valves that tolerate the pressure of 6000 psi. Of these four valves, two were ball valves and two were needle valves. The former ones were used for the injection of the solution and drainage of water and gas mixture after the experiment. The latter ones were used for two purposes: One was used to inject gas and the other was used to connect to the gas chromatograph device and gas sampling. Two vents were embedded at the outer wall of the reactor in order to control the reactor temperature by the inlet and outlet of the coolant by the passage of the refrigerant fluid. Ethylene glycol aqueous solution with the weight concentration of 50% was used as the coolant. Hydrate formation reactor and all refrigerant fluid connections and transfer tubes were well insulated. A Pt-100 temperature sensor is used with a precision of ± 0.1 K in order to reduce the energy loss. The reactor pressure was measured using a BD sensor with the precision of approximately 0.01 MPa. An oscillating mixer was used for the proper mixture in the hydrate formation reactor. A pump was used to create vacuum inside the reactor. A schematic of hydration formation device is shown in Figure 1.

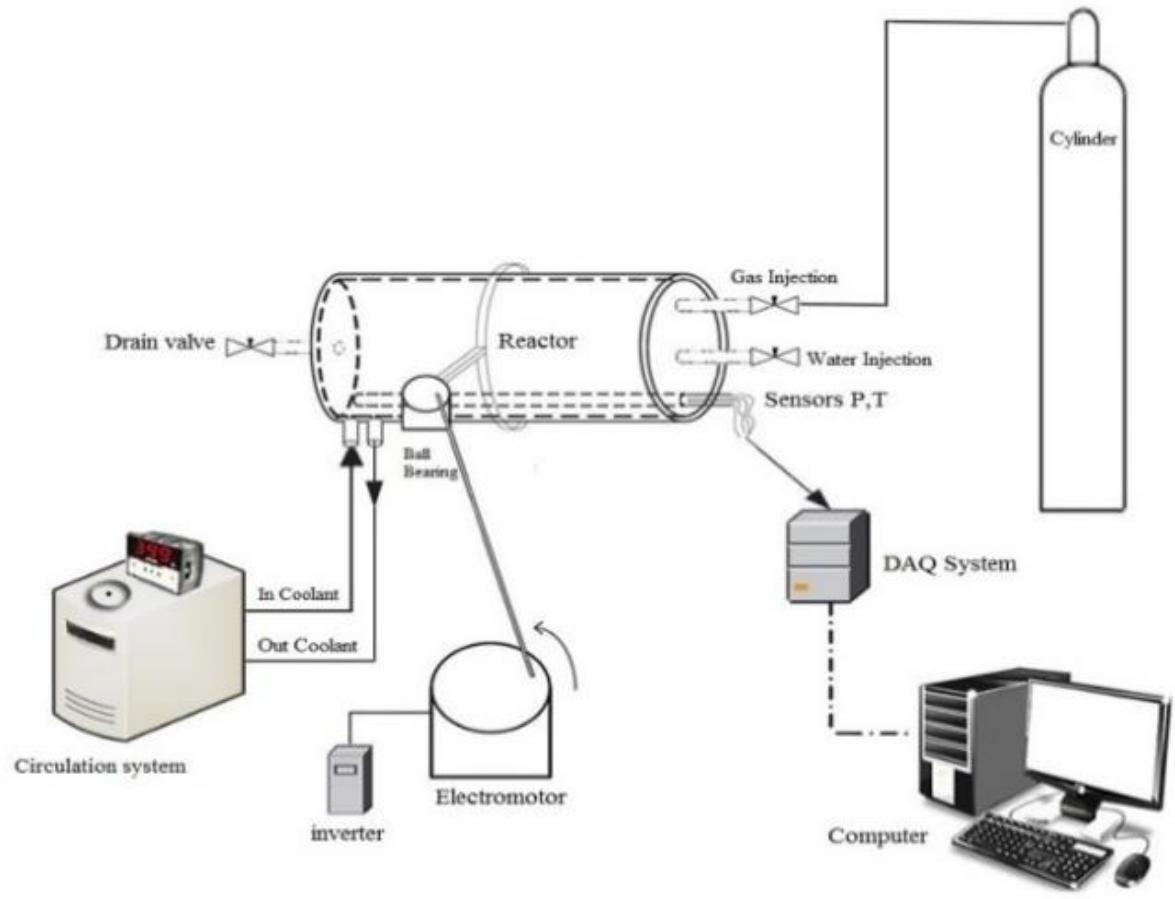

FIGURE 1 Schematic of the applicable hydrated device

Procedure

First, the reactor was washed with water by a continuous rotatory system for 10 minutes. Then it was rinsed by the distilled water. Vacuum pump was then used for 5 minutes to ensure the exit of intracellular air and

remaining water droplets. 100 cm^3 solution with 0.1 and 0.05% of graphene oxide nanoparticle weight concentration was prepared and injected into the cell. After setting the refrigerant temperature and stabilizing the temperature, CO_2 was injected at 40-bar initial pressure and oscillating mixer was turned off at fixed speed at the same time. As soon as the hydration formation process and CO_2 consumption began, the system pressure declined. Afterwards, pressure and temperature data were recorded on the computer at certain time intervals..

Model

Amount of gas consumed

Using the Peng-Robinson equation for calculation of gas consumed

$$P = \frac{RT}{v-b} - \frac{a\alpha}{[v(v+b)+b(v-b)]} \quad (1)$$

Calculations should be performed through rewriting the state equation in terms of the Z compressibility coefficient. Hence, Equation 2 is obtained with respect to Z by using the Peng-Robinson equation [24]:

$$Z^3 - (1 - B)Z^2 + (A - 2B - 3B)Z - (AB - B^2 - B^3) = 0 \quad (2)$$

$$A = \frac{a\alpha P}{R^2T^2} \quad (3)$$

$$B = \frac{bP}{RT} \quad (4)$$

$$a = 0.457235\frac{(RT_C)^2}{P_C} \quad (5)$$

$$b = 0.077796\frac{RT_C}{P_C} \quad (6)$$

$$\alpha = [1 + (m)(1 - (T/T_c)^{0.5})]^2 \quad (7)$$

$$m = 0.3796 + 1.458\,\omega - 0.16\,\omega^2 + 0.01667\,\omega^3 \quad (8)$$

where v is the molar volume, T_C and P_C are temperature and pressure at the critical point, respectively, R is the global gas constant, and ω is the acentric factor.

Using the determined Z at the initial and final (equilibrium) pressure and temperature, the initial and final (equilibrium) number of moles determine from Equations 9 and 10:

$$n_0 = \frac{P_0V_0}{Z_0RT_0} \quad (9)$$

$$n_e = \frac{P_eV_e}{Z_eRT_e} \quad (10)$$

$$\Delta n = n_0 - n_e \quad (11)$$

Equation 12 is used to calculate the standard volume of the CO_2 moles contained in hydrate.

$$V_{STP} = \frac{\Delta nRT}{P} \quad (12)$$

In Equation 12, the volume of CO_2 gas is calculated in standard conditions (1 bar and 15 °C).

2.1.2. Calculation of the storage capacity

$$SC = \frac{V_{STP}}{V_H} = \frac{\Delta n\, CO_2 RT_{STP}/P_{STP}}{V_H} \quad (13)$$

In this equation, V_H refers to the amount of hydrate produced (which is considered here 100 m^3).

Results and discussion

Statistical analysis of experimental results

The statistical results obtained from the experimental data using the Expert experiment design software are presented in Table 1. The response surface methodology (EMS) and the historical method were used for statistical analysis. In this case, four parameters affecting the process of CO_2 hydration in the presence of SDS surfactant and graphene oxide (GO) nanoparticles were randomly entered in the software. Parameter A was the reactor pressure, parameter B was the reactor temperature, parameter C was the SDS concentration, and parameter D was the GO concentration. The effects of change in the above parameters on R1 factor, the storage capacity of CO_2 in hydrate was investigated and recorded in the presence of SDS nanoparticles and SDS surfactant. This section presents the statistical analysis of the effect of regulatory parameters on storage capacity.

TABLE 1 The results of experiments to determine storage capacity

Run	Factor 1 A:Pressure bar	Fsctor 2 B:Temprature K	Factor 3 C:SDS ppm	Factor 4 D:GO -	Response 1 SC -
1	40.00	273.35	0.00	0.10	21.7434
2	40.00	275.95	0.00	0.10	20.6598
3	40.00	277.15	0.00	0.10	19.978
4	36.00	274.75	0.00	0.10	17.9364
5	36.00	275.95	0.00	0.10	16.1495
6	36.00	276.65	0.00	0.10	15.7036
7	40.00	274.85	0.00	0.05	28.3138
8	40.00	275.95	0.00	0.05	20.0843
9	40.00	276.95	0.00	0.05	18.652
10	36.00	275.65	0.00	0.05	21.6459
11	36.00	276.15	0.00	0.05	21.3049
12	36.00	277.15	0.00	0.05	21.0736
13	40.00	277.15	400.00	0.10	61.3216
14	36.00	276.95	400.00	0.10	52.6013
15	40.00	278.65	400.00	0.05	57.5503
16	36.00	277.15	400.00	0.05	51.9291

Statistical analysis of the parameters affecting storage capacity of CO_2 Hydrate

The experiments were carried out at different temperatures and pressures and different concentrations of nanoparticles and surfactant and the results are presented in Table 1.

After statistical analysis, a valid relation was found for estimating CO_2 storage capacity in hydrate.

$$SC = 38.74 + 1.85\,A - 2.67\,B + 18.06\,C - 1.19D \quad (14)$$

Figure 2 shows the effect of change in the reactor pressure on CO_2 storage capacity in hydrate. As shown, CO_2 storage capacity in hydrate increases as the reactor pressure increases. This may arise from increased solubility of CO_2 in water due to the increase in the reactor pressure, which in turn resulted in the acceleration of hydrate formation.

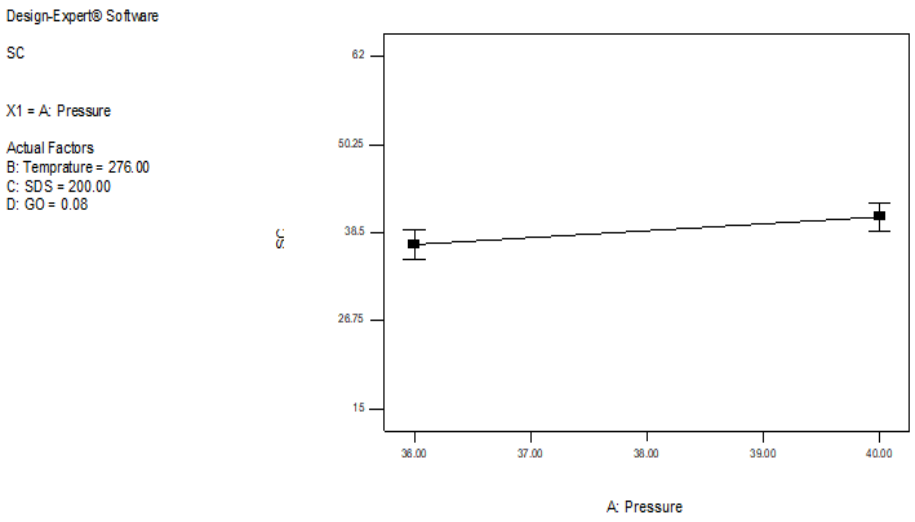

FIGURE 2 Changes in the storage capacity of CO_2 in hydrate as a function of the concentration of SDS

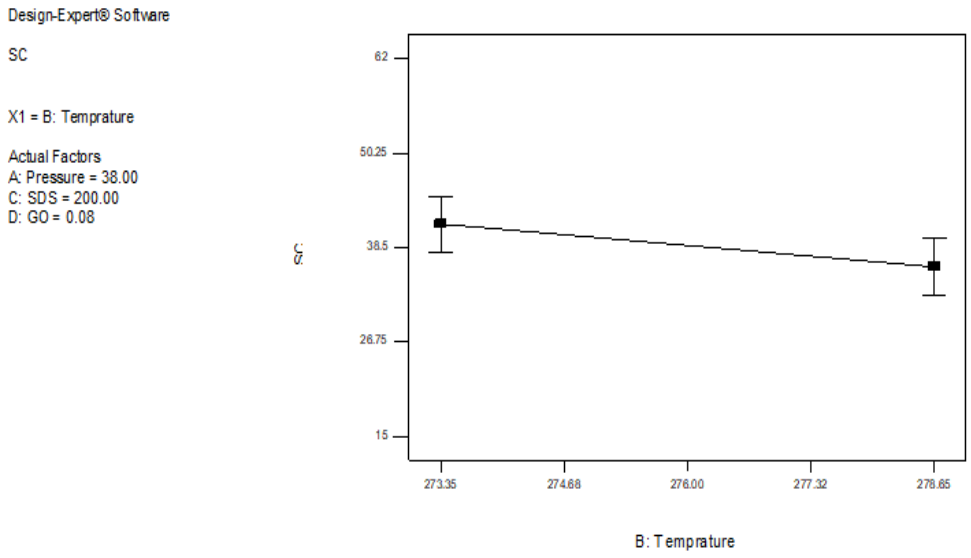

FIGURE 3 Changes in the storage capacity of CO_2 in hydrate as a function of the Temperature

Figure 4 shows the effect of changes in the SDS concentration on CO_2 storage capacity in hydrate. As shown, CO_2 storage capacity in hydrate increases significantly by increasing SDS concentration, since SDS sharply decreases the surface tension between water and gas, consequently resulting in a significant decrease in the resistance of gas penetration in water and hydrate.

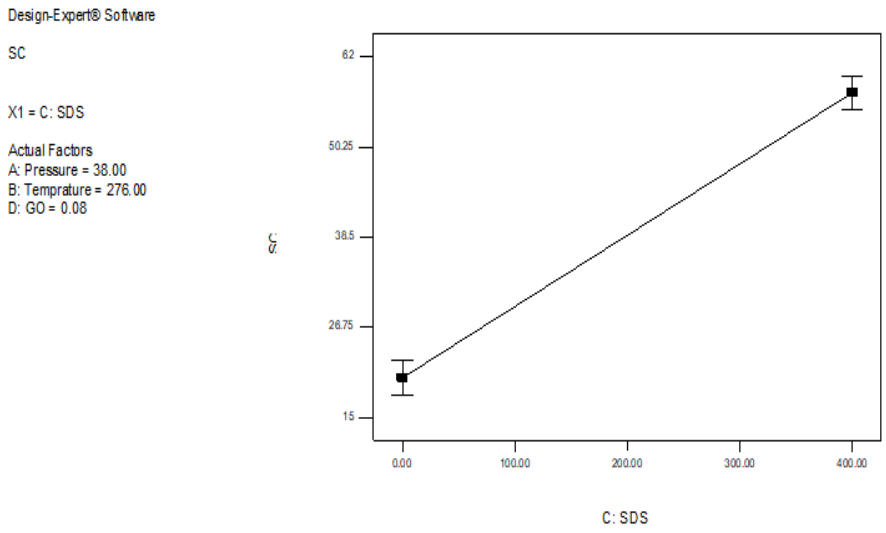

FIGURE 4 Effect of changes in SDS concentration on CO_2 storage capacity in hydrate

Figure 5 shows the effect of changes in the GO concentration on CO_2 storage capacity in hydrate. As shown, the storage capacity of CO_2 in hydrate does not change or even slightly decreases following the increase in GO concentration. At the hydrate formation temperature and pressure, hydrogen bonds produce cavities in water. Part of these cavities is occupied by GO, which reduces the penetration of CO_2 into hydrate and decreases the storage capacity.

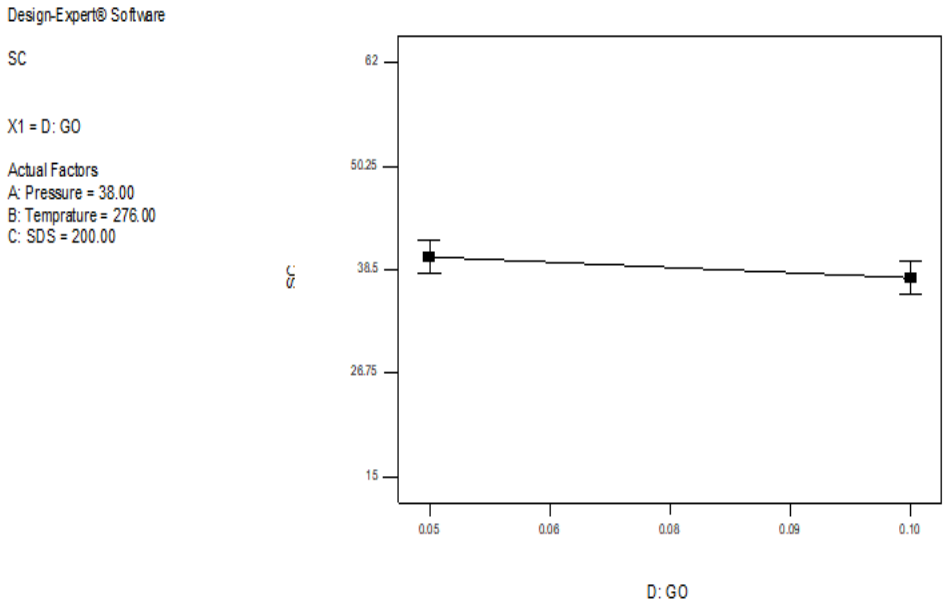

FIGURE 5 Effect of changes in GO concentration on CO_2 storage capacity in hydrate

In Figures 2-5, the effect of parameters influencing the storage capacity of CO_2 in hydrate was analyzed individually, irrespective of their interactions. According to Figures 1-4 and the statistical Equation 14, addition of SDS had the greatest impact on the storage capacity.

As shown in Figure 6, the simultaneous effect of temperature and pressure on CO_2 storage capacity in hydrates can be ignored.

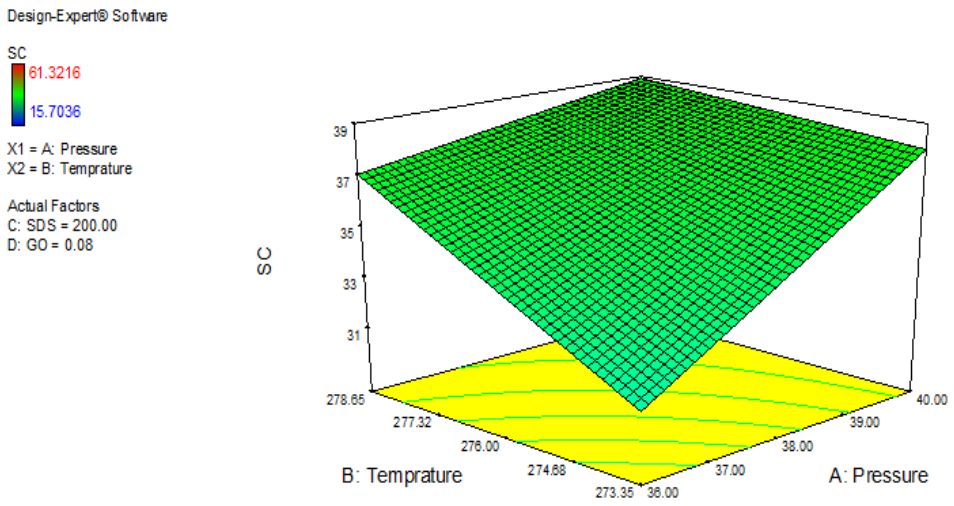

FIGURE 6 Simultaneous effect of reactor pressure and temperature on CO_2 storage capacity in hydrate

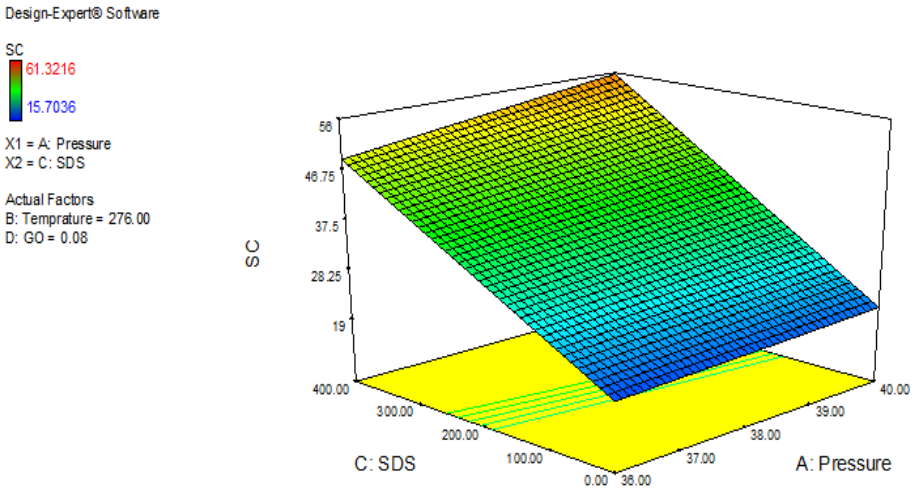

FIGURE 7 Simultaneous effect of SDS concentration and pressure on CO_2 storage capacity in hydrate

In Figure 7, the simultaneous effect of SDS concentration and pressure is plotted in 2D and 3D diagrams. As shown, the optimum CO_2 storage capacity in hydrate occurred at high pressures (>40 bars) and high SDS concentrations (>400 ppm).

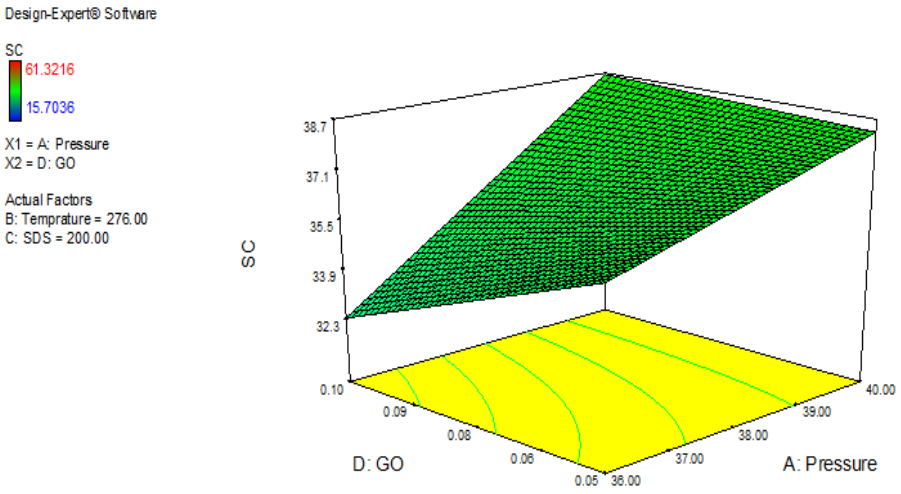

FIGURE 8 Simultaneous effect of GO concentration and pressure on CO_2 storage capacity in hydrate

Similar to Figure 5 (temperature and pressure), Figure 8 shows that pressure and GO concentration had no simultaneous effect on the CO_2 storage capacity. However, according to Figure 8, the CO_2 storage capacity in hydrate may increase at a pressure of >40 bars and a GO concentration of >0.1 wt%.

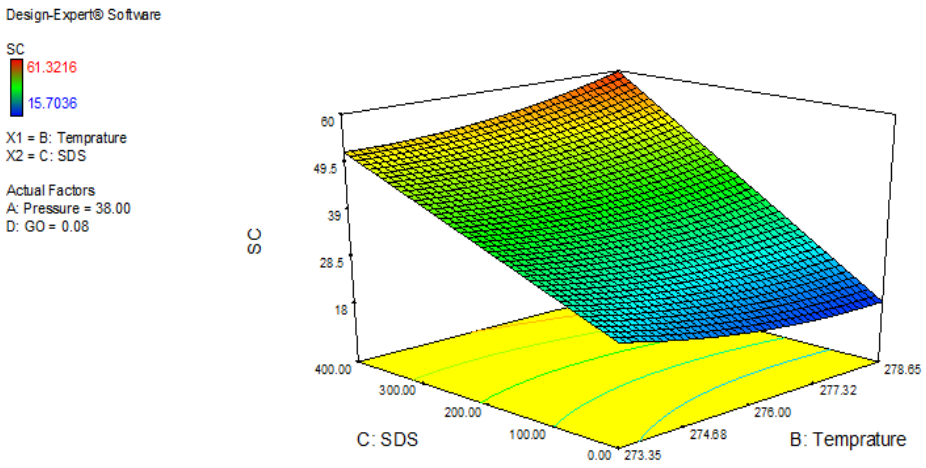

FIGURE 9 Simultaneous effect of SDS concentration and temperature on the CO_2 storage capacity in hydrate

As shown in Figure 9, the CO_2 storage capacity in hydrate is favorable in high temperature conditions (>273.23 K) and the presence of SDS (>400 ppm).

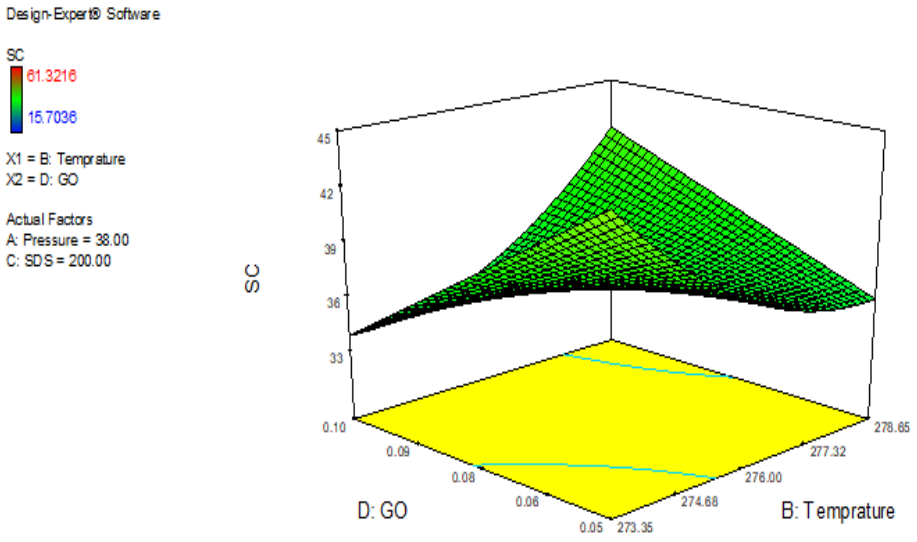

FIGURE 10 Simultaneous effect of GO concentration and temperature on the CO_2 storage capacity in hydrate

As in Figure 10, temperature and GO concentration had no simultaneous effect on the CO_2 storage capacity in hydrate under the experimental conditions.

Figure 11 shows the simultaneous effect of SDS and GO concentrations. As shown, the CO_2 storage capacity in hydrate increased at high SDS concentrations (>400 ppm) and high GO concentrations (>0.1 wt %).

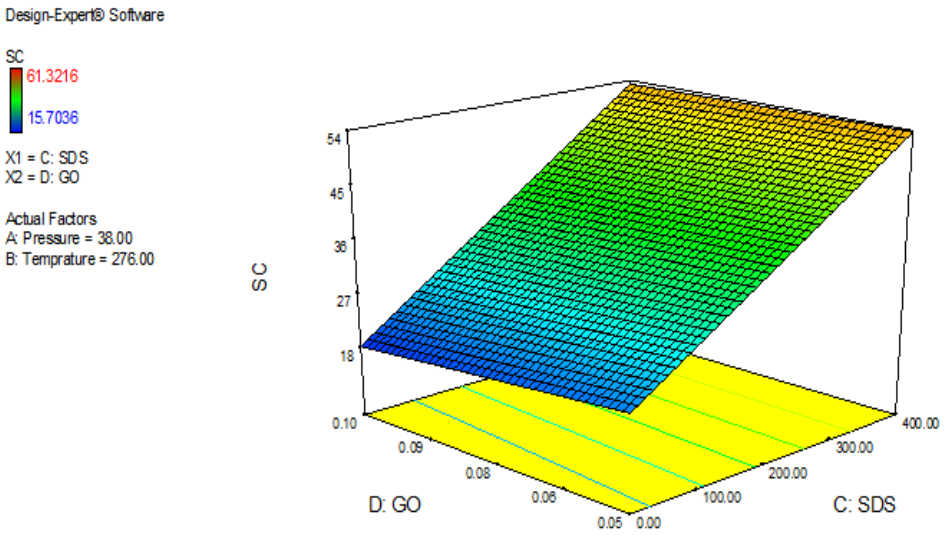

FIGURE 11 Simultaneous effect of GO and SDS concentrations on the CO_2 storage capacity in hydrate

Conclusion

The present study statistically analyzed the CO_2 storage capacity in hydrate in the presence of GO nanoparticles and SDS surfactant. The impact factor of parameters was statistically represented by an equation. The experiments were carried out in the range of pressure 36-40 bar, temperature range from 273.35 K to 278.65 K, in the presence of graphene oxide and sodium dodecyl sulfate. Experimental results showed that by increasing the pressure at constant temperature for net water, storage capacity increased by 11%, and the storage capacity increased by 14% by decreasing the temperature at the constant pressure (36 bar). Adding SDS, increases storage capacity by 26%, while adding graphene oxide, increased 4.2% of storage capacity. In addition, the pairwise simultaneous effect of parameters on storage capacity was investigated, which indicated that high concentrations of SDS had the greatest effect with increasing each of three parameters of temperature, pressure, and GO concentration.

Orcid:
Haniyeh Shamsin Beyranvand:
https://orcid.org/0000-0002-5364-6871

References

[1] A.A. Khokar, J.S. Gudmundssom, E.D. Sloan, *Fluid Ph. Equilibria*, **1998**, *150-151*, 383-392. [crossref], [Google Scholar], [Publisher]
[2] F. Zare Kazemabadi, A. Heydarinasab, A. Akbarzadeh, M. Ardjmand, *ARTIF CELL NANOMED B.*, **2019**, *47*, 3222-3230. [crossref], [Google Scholar], [Publisher]
[3] F. Wang, S. Fu, G. Guo, Z.Z. Jia, R.B. Guo, *Energy*, **2016**, *104*, 76-84. [crossref], [Google Scholar], [Publisher]
[4] A. Bozorgian, A. Samimi, *Int. J. New Chem.*, **2021**, *8*, 41-58. [crossref], [Google Scholar], [Publisher]
[5] A. Samimi, M. Samimi, *J. Eng. Indu. Res.*, **2021**, *2*, 1-6. [crossref], [Google Scholar], [Publisher]
[6] Z. Ma, P. Zhang, H. Bao, S. Deng, *Renew Sustain Energy Rev.*, **2016**, *53*, 1273-1302. [crossref], [Google Scholar], [Publisher]
[7] S. Muromachiu, A. Shijima, H. Miyamoto, R. Ohmura, *J. Chem. Thermodynamics*, **2015**, *85*,

94–100. [crossref], [Google Scholar], [Publisher]
[8] M. Yang, Y. Song, L. Jiang, Y. Zhao, X. Ruan, Y. Zhang, Sh. Wang, *Appl. Energy*, **2014**, *116*, 26–40. [crossref], [Google Scholar], [Publisher]
[9] W. Lee, Y.S. Kim, S.P. Kang, *Chem. Eng. J.*, **2018**, *331*, 1-7. [crossref], [Google Scholar], [Publisher]
[10] Y.S. Yu, S.D. Zhou, X.S. Li, S.l. Wang, *Fluid Ph. Equilibria*, **2016**, *414*, 23-28. [crossref], [Google Scholar], [Publisher]
[11] M. Yang, W. Jing, P. Wang, L. Jiang, Y. Song, *Fluid Ph. Equilibria*, **2015**, *401*, 27-33. [crossref], [Google Scholar], [Publisher]
[12] M. Zbuzant, *J. Eng. Indu. Res.* **2020,** *1*, 75-81. [crossref], [Google Scholar], [Publisher]
[13] A. Mohammadi, M. Manteghian, A. Haghtalab, A.H. Mohammadi, M. Rahmati-Abkenar, *Chem. Eng. J.*, **2014**, *237*, 387–395. [crossref], [Google Scholar], [Publisher]
[14] F. Zare Kazemabadi, A. Heydarinasab, A. Akbarzadehkhiyavi, M. Ardjmand, *Chem. Methodol.,* **2021**, *5*, 135-152. [crossref], [Google Scholar], [Publisher]
[15] Y. Raziani, S. Raziani, *J. Chem. Rev.,* **2021**, *3*, 83-96. [crossref], [Google Scholar], [Publisher]
[16] A. Ahmad, A. Sadrodin Reyazi, *J. Eng. Indu. Res.,* **2021**, *2*, 134-160. [crossref], [Google Scholar], [Publisher]
[17] Y. Raziani, S. Raziani, *Int. J. Adv. Stu. Hum. Soc. Sci.,* **2020**, *9*, 262-280. [crossref], [Google Scholar], [Publisher]
[18] N. Kayedi, A. Samimi, M. Asgari Bajgirani, A. Bozorgian, *S. Afr. J. Chem. Eng.,* **2021**, *35*, 153-158. [crossref], [Google Scholar], [Publisher]
[19] E. Amouzad Mahdiraji; M. Sedghi Amiri, *J. Eng. Indu. Res.* **2020,** 2, 111-122. [crossref], [Google Scholar], [Publisher]
[20] S. Delavari, H. Mohammadi Nik, N. Mohammadi, A. Samimi, S.Y. Zolfegharifar, F Antalovits, L. Niedzwiecki, R. Mesbah, *Chem. Methodol.,* **2021**, *5*, 178-189. [crossref], [Google Scholar], [Publisher]
[21] F. Rebout, *Journal of Engineering in Industrial Research,* **2020**, *1*, 19-37. [crossref], [Google Scholar], [Publisher]
[22] K.L. Han, *J. Eng. Indu. Res.,* **2020**, *1*, 38-50. [crossref], [Google Scholar], [Publisher]
[23] F. Gharekhani Kasa, *J. Eng. Indu. Res.,* **2020,** *1*, 51-74. [crossref], [Google Scholar], [Publisher]

How to cite this article: Haniyeh Shamsin Beyranvand*, Hamid Sarlak. Effects of Graphene oxide (GO) nanoparticle and SDS on storage capacity of CO_2 in hydrate. *Eurasian Chemical Communications*, 2021, 3(4), 233-243. **Link:** http://www.echemcom.com/article_128685.html